OBSERVATION OF ASPHERICAL PARTICLE ROTATION IN POISEUILLE FLOW VIA THE RESISTANCE PULSE TECHNIQUE

I. Application to Human Erythrocytes

D. C. GOLIBERSUCH

From the General Electric Research and Development Center, Schenectady, New York 12345

ABSTRACT The resistance pulse detector (Coulter counter) has been widely applied to the problem of determining the volumes of insulating particles in electrolyte solutions. This technique is based on the simple relationship, $\Delta R/R = fv/V$, between the fractional resistance change $\Delta R/R$ and the ratio of particle volume v to pore volume V. The proportionality constant f is a function of particle shape and orientation. Direct observation of the expected resistance anisotropies for aspherical particles is reported here. As predicted by simple hydrodynamic theory each individual resistance pulse has a periodically varying amplitude as it traverses a long pore in the shear field of Poiseuille flow. Characteristics of the particle motion allow improved volume distribution determinations by properly accounting for the shape factor. Application is made to normal human erythrocytes and a *gaussian volume distribution* with a coefficient of variation $\sim 19\%$ is found. The electrical shape effect for erythrocytes is consistent with an oblate ellipsoidal particle with a diameter-to-thickness ratio of 4. Analysis of the data indicates that the convergent entrance flow orients the cells so that they enter the pore with their axis of symmetry perpendicular to the pore axis.

I. INTRODUCTION

The change in resistance of an electrolyte-filled pore caused by the presence of an insulating particle is proportional to the particle's volume. This effect has been widely exploited to count and size particles of biological interest.[1] In addition to the volume dependence, however, the amplitude of the resistance change also depends on the shape and orientation of the particle. This fact has been ignored by many workers even though it can lead to significant errors in the inference of volume distributions.

Through the use of long pores I have been able to observe the shape and orientation effects directly. This is done by observing a given particle for a time comparable

[1] Coulter Counter Bibliography, Coulter Electronics, Inc., Hialeah, Fla. Unpublished.

with the period of rotation of the particle. This rotation results from the shear present in the fluid flow.

In section II of this paper I describe the electrical shape effect and then review some results of the theory of particle motion in laminar fluid flow in section III. Several consequences of this motion are shown in section IV to allow an accurate determination of aspherical particle volume. In sections V and VI these considerations are applied to an experimental study of normal human erythrocytes. Discussion and analysis of these experiments is continued in section VII.

II. THE ELECTRICAL SHAPE EFFECT

Maxwell (1) was the first to calculate the resistivity of a suspension of insulating particles. For the case of a single small particle within a pore the dilute limit of Maxwell's expression is appropriate and we obtain

$$\frac{\Delta R}{R} = fv/V \tag{1}$$

Here ΔR is the difference between the resistance of the pore in the presence and absence of a particle, R is the resistance of the pore alone, v is the volume of the particle, and V is the volume of the pore. The shape factor f for the case of spheres considered by Maxwell has the value $3/2$. This factor of $3/2$ has been verified for the case of small spherical particles by the experimental work of Gregg and Steidley (2) and Grover et al. (3). Smythe (4) specifically considered the problem of an insulating sphere in a conducting cylinder for all values of the ratio of particle to pore diameter d/D. His numerical results reduce to the Maxwell limit for small particles and in addition are in excellent agreement[2] with the experiments of Gregg and Steidley (2), Grover et al. (3), and DeBlois and Bean (5) over the entire range of d/D. Fricke (6) extended Maxwell's treatment to consider spheroids and in particular calculated the shape factor for ellipsoids of revolution. Velick and Gorin (7) extended this work to include the general elliposid. Smythe (4) also obtained numerical solutions for two special cases of ellipsoids of revolution. His work indicates that as a general rule of thumb the Maxwell limit (Eq. 1) with f as determined by Fricke and Velick and Gorin will be sufficiently accurate (better than 1 %) as long as the particle dimension is less than one-third the pore diameter. Recently Bean[2] has pointed out that the shape factor for ellipsoids of revolution is simply related to the extensively tabulated demagnetization factors (8, 9). He obtains

$$f_{\parallel} = \frac{1}{1 - n_{\parallel}} \quad \text{and} \quad f_{\perp} = \frac{1}{1 - n_{\perp}}, \tag{2}$$

[2] Bean, C. P. Private communication.

with

$$n_\parallel + 2n_\perp = 1. \tag{3}$$

Here $f_\parallel$ and $n_\parallel$ are the electrical shape factor and demagnetization factor for the case of a field directed parallel to the axis of revolution and $f_\perp$ and $n_\perp$ are the corresponding factors for the perpendicular orientation. By symmetry it is clear that for a particle with an axis of symmetry we obtain

$$\frac{\Delta R}{R} = [f_\perp + (f_\parallel - f_\perp)\cos^2\alpha]v/V, \tag{4}$$

where α is the angle between the field and the axis of revolution.

In Fig. 1 I have plotted the values of $f_\parallel$ and $f_\perp$ for ellipsoids of revolution as a function of γ_E. This latter parameter is defined as the ratio of the axis of revolution to the equatorial axis of the particle. The ratio, $f_\parallel/f_\perp$, is plotted in Fig. 2. This quantity tells us the extent by which the volume distribution for a suspension of identical ellipsoids will be artificially broadened if various particles were to assume all possible orientations. Of particular interest in this paper is the case of human erythrocytes which have a shape close to that of an oblate ellipsoid with $\gamma_E = 0.25$, that is a diameter-to-thickness ratio of 4. For this case we see that the shape factor range is roughly a factor of 3. Another parameter of particular interest is the average shape factor f_{avg} for the case of a randomly oriented ensemble of particles. The ratio of this quantity to that for a sphere is plotted in Fig. 3. We note that for prolate ellipsoids (rod-like) the maximum difference between f_{avg} and $f = 3/2$ for spheres is

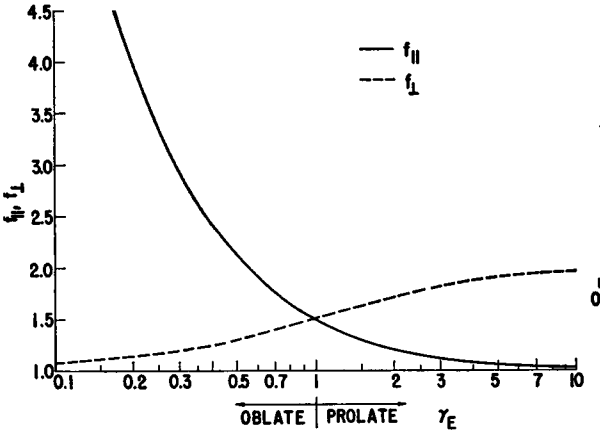

FIGURE 1

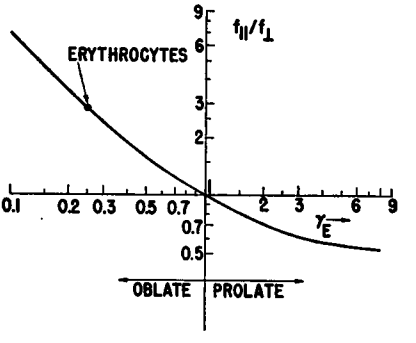

FIGURE 2

FIGURE 1 The electrical shape factors, $f_\parallel$ and $f_\perp$ for ellipsoids of revolution as a function of γ_E, the ratio of particle axis of revolution to equatorial diameter.

FIGURE 2 The ratio, $f_\parallel/f_\perp$ vs. γ_E. The point for erythrocytes assumes a diameter-to-thickness ratio of 4, i.e., $\gamma_E = 0.25$.

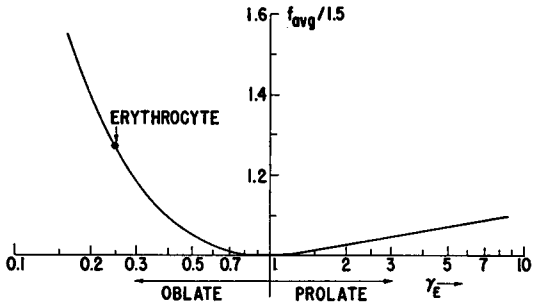

FIGURE 3

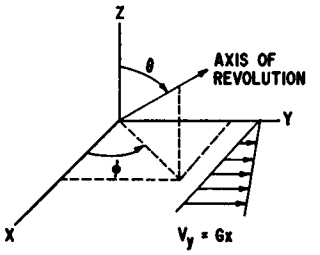

FIGURE 4

FIGURE 3 The ratio of the average shape factor for a randomly oriented ensemble of identical ellipsoids of revolution to the factor for spheres, $f = 1.5$ as a function of γ_E.
FIGURE 4 The polar coordinates used to describe the orientation of the particle's axis of revolution relative to the direction of fluid velocity and shear.

only 11%. For typical rod-shaped bacteria with axis ratios of 2 or 3 to 1 the difference is only 3–5%. The situation for oblate ellipsoids (disk-like) is quite different. For human erythrocytes we would expect f_{avg} to deviate by some 27% from the value appropriate for spheres.

III. MOTION OF AN ASPHERICAL PARTICLE IN A SHEAR FIELD

The equations of motion for a rigid ellipsoid of revolution moving in a uniform shear field at low Reynolds's number have been solved exactly by Jeffery (10). He found that the particle has a translational velocity identical with the local undisturbed fluid velocity. In addition the particle rotates such that the axis of symmetry moves in one of the orbits described by the following equations.

$$\tan \Phi = \gamma_H \tan (2\pi t/T + C_1), \tag{5}$$

$$\tan \theta \, (\gamma_H^2 \cos^2 \Phi + \sin^2 \Phi)^{1/2} = C_2, \tag{6}$$

$$T = \frac{2\pi}{G} \frac{1 + \gamma_H^2}{\gamma_H}. \tag{7}$$

The angles θ and Φ are the polar coordinates indicated in Fig. 4, γ_H is the hydrodynamic shape factor defined as the ratio of the axis of revolution to the equatorial axis,[3] G is the magnitude of the shear, and C_1 and C_2 are constants which define a particular orbit. The Jeffery solutions have been accurately verified experimentally by Trevelyan and Mason (11). Bretherton (12) has theoretically demonstrated that

[3] The definitions of γ_E and γ_H are identical. The distinction is made to allow describing a real particle in terms of an equivalent ellipsoid of revolution so as to account for both its electrical and hydrodynamic properties. The effective values of γ_E and γ_H so obtained may differ.

the rotation of almost all rigid bodies of revolution in a simple uniform shear is identical with some ellipsoid of revolution.

In the case of Poiseuille flow in tubes the fluid velocity v is given by

$$v(r) = v_0 [1 - (r/R)^2], \tag{8}$$

where v_0 is the axial velocity, R is the tube radius, and r is the radial position. This gives rise to a radial shear G of magnitude.

$$G(r) = dv/dr = -2v_0 r/R^2. \tag{9}$$

This, of course, differs from the simple uniform shear considered by Jeffery. Goldsmith and Mason (13), however, have observed in experimental work that the particle rotations are still accurately described by the Jeffery equations if γ_E is empirically determined by the period (Eq. 7) rather than the geometrical definition.

IV. TECHNIQUE FOR ACCURATE VOLUME DETERMINATION

The particle orbits described in the last section (Eqs. 5–7) have several important characteristics: (*a*) the orbits are stationary, (*b*) the orbits are periodic, and (*c*) twice in each period the particle will be oriented with its axis of symmetry perpendicular to the flow. In an elegant demonstration of the power of symmetry, Bretherton (12) has shown that as long as a basic reversing mechanism exists and inertial forces can be neglected, then these characteristics will be exhibited by any particle with an axis of revolution moving in any flow (bounded or unbounded) as long as it is unidirectional.

These periodic rotations are reflected as periodic variations in the shape factor f and in turn the amplitude of the resistance pulse. In Appendix I, I show that the shape factor extrema are realized for $\Phi = 0, \pi/2, \pi, 3\pi/2, \ldots$. For $\Phi = 0, \pi, 2\pi, \ldots$, the axis of symmetry is perpendicular to the field and $f = f_\perp$. For an oblate ellipsoid this corresponds to an absolute minimum in the resistance pulse while for a prolate ellipsoid this corresponds to an absolute maximum. For $\Phi = \pi/2, 3/2\,\pi, \ldots$ relative extrema are found whose amplitude depends on the particular orbit. For oblate ellipsoids this will be a relative maximum and for prolate ellipsoids a relative minimum. These observations are illustrated in Fig. 5 where the results of a computer evaluation of the orbital and shape factor equations are shown for the case of an oblate ellipsoid with $\gamma_E = \gamma_H = 0.25$ and three particular initial orientations.

V. EXPERIMENTAL OBSERVATIONS OF NORMAL HUMAN ERYTHROCYTES

The experimental arrangement is described schematically in Fig. 6. The device is operated in an approximately constant current mode with the load resistance,

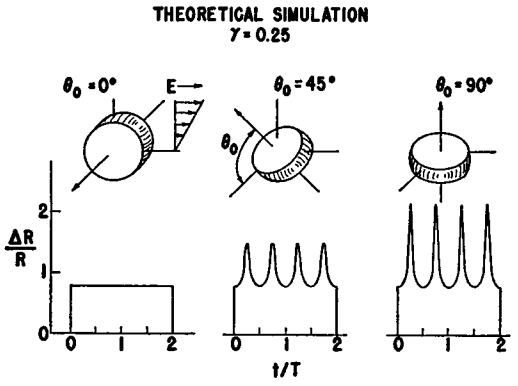

FIGURE 5

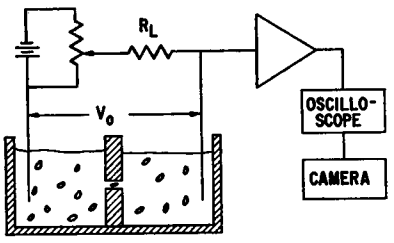

FIGURE 6

FIGURE 5 Computer evaluation of Eqs. 4–7 for a particle with $\gamma_B = \gamma_H = 0.25$ and three different initial orientations. In each case $\Phi_0 = 0$. The ordinate scale is fixed relative to the value of $\Delta R/R$ which would obtain with a sphere of identical volume. For convenience the particle's radial position and the pore length are such that the particle completes exactly two complete revolutions as it traverses the length of the pore. Note that for an oblate ellipsoid the minimum pulse amplitudes are independent of initial orientation.

FIGURE 6 Schematic diagram of the experimental arrangement.

$R_L \gg R$, the pore resistance. The pores were constructed by drawing down lengths of capillary tubing and then grinding thin slices with the required diameter until the desired length was obtained. For ease of handling the finished capillary sections were then epoxy bonded to Plexiglas disks with a 1.7 cm outer diameter and a small central hole. The composite disks were mounted between the two halves of the experimental chamber using "O" rings. The Plexiglas chamber contained a fluid volume of $\sim$1 cm^3 on each side of the pore. The electrodes were Ag-AgCl.

The cells were obtained by finger prick and immediately diluted by a factor of 20,000 in buffered saline[4] with 0.5% human albumin. The albumin was found necessary to preserve the shape of the cells. (In saline alone the cells were observed to become quickly crenated, then spherical, and ultimately hemolysed at these high dilutions. The cause of this effect is unknown although trace cell poisons are suspected. (The minute amount of AgCl soluble in water was identified as one agent in control experiments. Ions of heavy metals are known as potent antimicrobial agents (14). Even without AgCl, erythrocytes were observed to deteriorate somewhat more quickly in the Plexiglas experimental cell than controls in glass vials.) In spite of all precautions the cells began to deteriorate after about 45 min. During the run a small sample of erythrocytes was periodically withdrawn from the experimental cell and checked microscopically. As soon as a noticeable number of the cells were observed to deviate from the perfect biconcave disk shape the experiment was stopped.

[4] Baltimore Biological Laboratory Earle's solution (Div. of Becton-Dickinson and Co., Cockeysville, Md.). Ingredients per liter: NaCl, 6.8 g; KCl, 0.4 g; $CaCl_2$, 0.2 g; $MgSO_4 \cdot 7H_2O$, 0.2 g; NaH_2PO_4, 0.125 g; dextrose, 1 g; $NaHCO_3$, 2.2 g; and phenol red, 0.02 g.

Several examples of the pulses observed during one run are reproduced in Fig. 7. For this data the experimental parameters were as follows: pore diameter = 42 μm and length = 420 μm, R_L = 1 MΩ, V_0 = 5 V, R = 200 kΩ, amplifier gain = 100, and upper frequency 3 dB point determined by input RC was ~50,000 Hz. A pressure differential of ~1 cm of H_2O was used to drive the particles through the pore. The system was not directly calibrated because of the lack of test particles of suitable known volume. The observed pulse amplitude, however, can be accurately related to particle volume by the expression:

$$\Delta V' = V_0 fv \left(\frac{\pi}{4} D^2 L'\right)^{-1} G \frac{R_L}{R + R_L}, \tag{10}$$

where $\Delta V'$ is the observed pulse amplitude, G is the amplifier gain, and the effective length, $L' = L + 0.8D$. (The effective length is used to approximately account for edge effects.) With the above parameters for this particular run we have $fv = 1.49\ \Delta V'\ \mu m^3$ with $\Delta V'$ in millivolts.

From the photographs, the minimum and maximum amplitudes for each pulse,

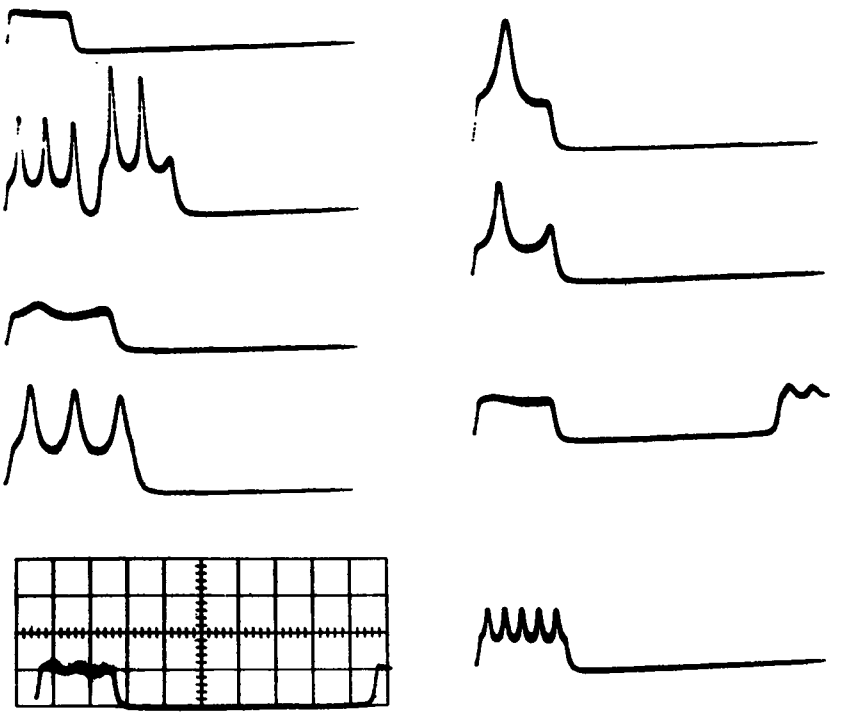

FIGURE 7 Resistance pulse signatures obtained for a specimen of normal human erythrocytes. The pore diameter and length were 42 and 420 μm, respectively. The oscilloscope scale factors are the same for all traces, viz., 50 mV/cm by 10 ms/cm. The second trace from the top on the left arises from two cells in near coincidence.

were measured. These data were used to prepare histograms such as Fig. 8. Only those pulses which exhibited a clearly defined minimum *and* maximum were plotted. These data are shown replotted on probability paper in Fig. 9. The coefficient of variation (C.V.) of the minimum amplitudes for this run was 18.8%. The mean minimum amplitude of 4.8 units corresponds to an electrical volume of 76.5 μm^3 assuming an oblate ellipsoid with $\gamma_E = 0.25$ and $f_\perp = 1.17$. As expected the amplitude distribution obtained from the minima is narrow and gaussian. By contrast the maximum amplitude distribution is broadened by roughly a factor of three and is strongly skewed to the right. Both the mean and the mode are shifted to larger amplitude.

As a final illustration of the data, I have plotted in Fig. 10 the maximum amplitude as a function of minimum amplitude for each pulse. The lower line is the locus of points for identical minimum and maximum amplitude. (The data for spherical particles would all fall on this line.) The upper line is the locus of points for particles with $\gamma_E = 0.25$ whose orbits include both extremes of orientation, that is $f = f_\parallel$ and $f_\perp$ both occur. The fact that essentially all the data points fall between the two solid lines indicates that the electrical shape factor for erythrocytes is well described by our assumption of an oblate ellipsoid with $\gamma_E = 0.25$, in other words, an ellipsoid with a diameter-to-thickness ratio of 4.

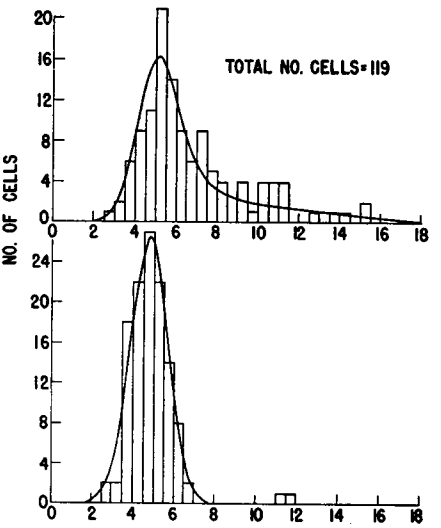

FIGURE 8 Minimum (bottom) and maximum (top) pulse amplitude histograms for a sample of normal human erythrocytes. The data are from the same run as the pulses of Fig. 7. The solid curve on the minimum amplitude plot is a gaussian with $A_0 = 4.8$ and $\sigma = 0.9$ which has been normalized so as to have the same area as the histogram, viz., 59.5. The theoretical curve on the maximum amplitude plot is explained in the text. The abscissa scales are such that 1 unit corresponds to 12.5 mV as seen on the oscilloscope traces of Fig. 7.

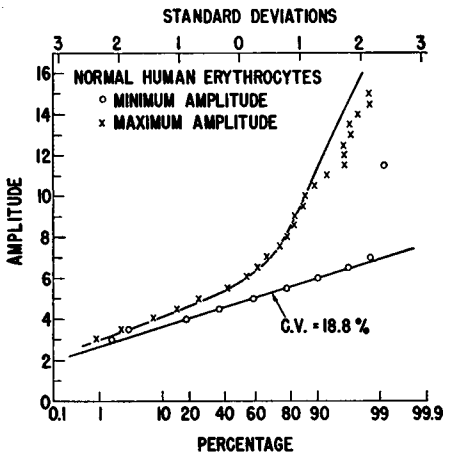

FIGURE 9

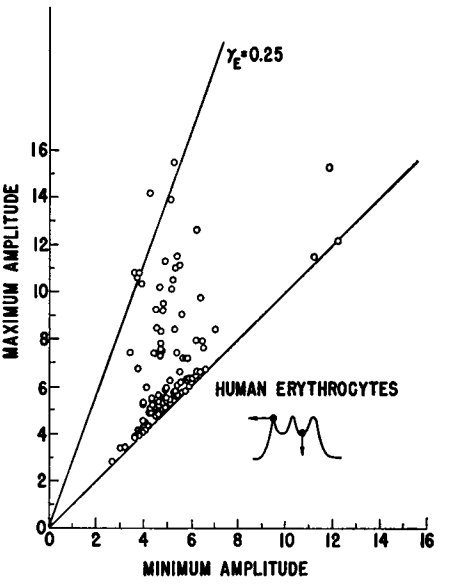

FIGURE 10

FIGURE 9 The minimum and maximum amplitudes plotted on probability paper. The data are from the same run as Figs. 7 and 8. The lower solid line fit to the minimum amplitude data represents a gaussian with $A_0 = 4.8$ and $\sigma = 0.9$. The upper solid curve is a theoretical fit to the maximum amplitude data as explained in the text.

FIGURE 10 Maximum amplitude vs. minimum amplitude. The data are the same as that of Figs. 8 and 9. The lower solid line is drawn for equal minimum and maximum amplitude. The upper line is drawn for the ratio of maximum to minimum amplitudes equal to $f_\perp/f_\parallel$ for particles with $\gamma_E = 0.25$.

VI. THE MAXIMUM AMPLITUDE DISTRIBUTION AND ORIENTATION EFFECTS

It is impossible at this time to predict with certainty the shape of the maximum amplitude distribution. Such a calculation requires knowledge of the distribution of particle orientations at the time the maximum amplitude measurements are made. In terms of the polar coordinates we must know the distribution of θ's when $\Phi = \pi/2$. Alternatively if we knew the distribution of orientations at some time or spatial location within the pore such as the entrance plane it would be possible to calculate the θ distribution for $\Phi = \pi/2$ using the orbital equations. A priori, the only sure statement that can be made is that the particles are undoubtedly randomly oriented sufficiently far from the pore entrance. Unfortunately very little is known of the particle motion in the convergent entrance flow. In an effort to understand the implications of the maximum amplitude distribution seen in the histogram of Fig. 8 let us now examine the consequences of two simple assumptions regarding the distribution of particle orientations within the pore.

First let us consider the distribution which would occur if the particles were

randomly oriented at the time of maximum amplitude determination. The shape factor for maximum amplitude orientation (that is, $\Phi = \pi/2$) is determined by

$$f = f_\perp + (f_\parallel - f_\perp) \sin^2 \theta. \tag{11}$$

If we now assume that all θ are equally likely we will have

$$P(f)\, df = P[\theta(f)] \frac{d\theta}{df} df = \frac{1}{\pi} \left(\frac{df}{d\theta}\right)^{-1} df, \tag{12}$$

since $P(\theta)d\theta = \pi^{-1}d\theta$ by assumption.

Performing the differentiation and eliminating θ with Eq. 11 we obtain

$$P(f)\, df = \frac{1}{2\pi} \frac{df}{(f - f_\perp)^{1/2}(f_\parallel - f)^{1/2}}. \tag{13}$$

This is a symmetric bimodal distribution with peaks at $f = f_\perp$ and $f_\parallel$ and disagrees markedly with the observed distribution of Fig. 8. To overcome this strong "density of states" effect of Eq. 11 and obtain the skewed distribution actually observed requires that the true angular distribution $P(\theta)$ be heavily weighted in favor of θ near 0 and π.

A more realistic assumption of the distribution of particle orientations within the pore can be obtained by examination of the pulses of Fig. 7. Note that all the pulses begin with an amplitude close to the minimum amplitude. In other words, essentially all of the cells enter the pore with their axis of symmetry perpendicular to the flow, i.e., $\Phi_0 = 0$. We still do not know, however, the distribution of the entrance θ_0's. In our second effort to account for the distribution of maximum amplitudes let us assume that the θ_0 orientation is random, i.e., $P(\theta_0)\, d\theta_0 = (\pi)^{-1}\, d\theta_0$. With this assumption the distribution of θ's at the point where the maximum amplitude determination is made, i.e., $\Phi = \pi/2$ will not be uniform as a consequence of the orbital characteristics. From Eq. 6 we have

$$\tan \theta = \gamma_H \tan \theta_0. \tag{14}$$

Differentiating Eq. 14 we obtain

$$P(\theta)\, d\theta = P(\theta_0(\theta)) \frac{d\theta_0}{d\theta} d\theta = \frac{\gamma_H}{\pi} \frac{1 + \tan^2 \theta}{\gamma_H^2 + \tan^2 \theta} d\theta. \tag{15}$$

This is a skewed unimodal distribution with a peak at $\theta = 0$. Repeating the calculation of the last paragraph using the distribution for $P(\theta)$ given by Eq. 15 and transforming to a more convenient variable, $f' = (f - f_\perp)/f_\parallel - f_\perp)$, we obtain

$$P(f')\, df' = \frac{\gamma_H}{\pi} \frac{df'}{[\gamma_H^2 + (1 - \gamma_H^2)f']f'^{1/2}(1 - f')^{1/2}}. \tag{16}$$

This distribution is still bimodal, but is skewed and for $\gamma_H < 1$ weighted toward $f' = 0$, i.e., $f = f_\perp$. As described in Appendix II Eq. 16 is then convoluted with the gaussian distribution obtained from the minimum amplitude data to obtain the theoretical maximum amplitude distribution. The result, for $\gamma_E = \gamma_H = 0.25$, is plotted in Figs. 8 and 9. This is a skewed, unimodal distribution with both the mean and the mode shifted to larger amplitude relative to the minimum amplitude distribution. The excellent agreement with experiment suggests that the distribution of initial orientations assumed here may be a close approximation to the truth.

VII. DISCUSSION

One of the most significant results obtained here is that the distribution of normal erythrocytes as determined from the minimum pulse amplitudes is found to be narrow and gaussian. By contrast the maximum amplitude distribution is found to be strongly skewed and broadened.

Numerous examples of skewed erythrocyte amplitude distributions have been reported in the literature. In all previous work the pores employed have been short compared with the length necessary for the particles to complete a revolution. In addition, in most work the measurement recorded is the maximum pulse amplitude which occurs during passage through the pore. One important question is can these distributions be accounted for by shape effects. Efforts in the literature to explain the skewed erythrocyte distributions form a potpourri of every conceivable contributory factor. A partial list includes: distribution is truly bimodal with subpopulations of old and new cells (15, 16), shape and orientation (17), cell distortion by fluid shear (18), distortion of cells by electric current (16), distortion of cells by storage or improper diluting medium (17), inhomogeneous electric fields within the orifice (19), artifact resulting from slow electronics response (20), orifice geometry artifact, "anomolous osmotic effect of hemoglobin" (21), etc.

Exceptional examples of normal erythrocyte distributions are found in the work of Shank et al. (18) and Miller and Wuest (19). These authors were careful to avoid trivial problems such as crenation and sphering in improper media and electronic response time artifacts. Both used a director to fix the radial position of the cells within the pore. They found that cells traversing on axis resulted in a narrow normal distribution (Shank et al., C.V. = 20%; Miller and Wuest, C.V. = 14%). On the other hand, cells traversing near the pore edge yielded a somewhat skewed and broadened distribution with a larger mean amplitude. Without a director so that cells entered at all radial positions a broad skewed distribution was found. Shank et al. attempted to account for these observations by arguing that the nonrigid erythrocyte is variously elongated at different radial positions "due to the rapid acceleration as they approach the orifice" (18).

In an effort to simplify the problem Miller and Wuest (19) repeated their ex-

periments with spherical particles. For various orientations of the director they observed normal distributions with essentially identical standard deviations. The mean values of these distributions, however, depended on director orientation. A minimum mean value was obtained for the case where the particles traversed the pore on axis and progressively larger mean values were obtained as the particles traversed the pore closer to its edge. In the absence of a director a skewed distribution was observed which appears to be a simple convolution of these normal distributions weighted such that particles preferentially enter the pore on axis. These authors argued that the observed pulse height distribution depends on the radial position of the particles because of inhomogeneous fields near the pore edge. Based on the following considerations I believe this argument to be qualitatively correct. (*a*) The electric field near the entrance will be inhomogeneous which will cause an inhomogeneous current density. (*b*) Current conservation tells us that the net current across the entrance plane must be the same as that across a plane further in the pore where the current density is uniform. (*c*) Since the net current is conserved there must be regions of current density at the entrance plane both higher and lower than the average current density. (*d*) For tubes of constant current the resistance pulse is to a first approximation proportional to the square of the local current density. Grover et al. (3) have attempted to make the first part of this argument quantitative although their approximate solution of the potential problem does not strictly conserve current. The observations of Miller and Wuest (19) with spheres are in agreement with DeBlois[5] who uses long pores and electronic delay triggering so as to sample the pulse amplitude far from the entrance. DeBlois is then able to obtain extremely sharp distributions, e.g., a coefficient of variation of 1.5% with 0.357 μm particles!

With the potential importance of the effect of the inhomogeneous field near the pore entrance in mind let us now return to the question of the effect of erythrocyte shape on the distribution. The fact that a normal distribution is found for erythrocytes which traverse the pore on axis led Shank et al. (18) and Miller and Wuest (19) to propose that all the cells must enter the pore with the same orientation. As mentioned earlier our knowledge of the particle motion in the convergent entrance flow is limited. The symmetry argument (section IV) in favor of stationary orbits breaks down in this region since the flow is not unidirectional. Bretherton (12) has considered particle motion in convergent flow and finds that particle orientation is indicated. Indeed, as already discussed direct evidence is found in the present work (Fig. 7) that the particles are oriented on entrance into the pore with their axis of symmetry perpendicular to the flow. Further indirect evidence for this orientation was obtained from analysis of the maximum amplitude distribution as discussed in section VI.

In summary, evidence suggests that in many situations erythrocytes will be strongly

[5] DeBlois, R. W. Private communication.

oriented by the convergent entrance flow so as to enter the pore with a fixed shape factor. Thus the aspherical nature of the particle will not affect the volume distribution obtained with the usual short pores except as to determine the appropriate proportionality constant between pulse height and volume. By contrast, if the radial position of the particles is not fixed then one can expect considerable distortion of the distributions because of the inhomogeneity of the electric field within the measurement region. Some questions remain. Miller and Wuest (19) do not obtain a simple distribution for erythrocytes directed near the pore edge. They suggest that cell distortion may cause this. It would be interesting to explore further the question of orientation of such cells by combining a director and the long pore geometry of the present work. Another reservation must be held in comparing the present work with some previous work where very high Reynolds's number flows were employed. It is likely that in these circumstances turbulence was present which might tend to randomize the particle orientation and thus cause particle shape to distort the distributions.

Qualitatively, the experimentally observed amplitude variations (Fig. 7) are in very good agreement with those theoretically expected on the basis of Jeffery's equations (Fig. 5). It is apparent that the resistance pulse technique may be useful in the general rheological study of low viscosity, moderate Reynolds's number environments where the particle motion is too rapid for study by the direct microscopic techniques of Mason and collaborators (11, 13, 22). The existence of radial migration or nonstationary orbits is of concern in studies of small particle motion in tube flow. In many cases, these two effects can be rigorously ruled out by the aforementioned symmetry arguments of Bretherton. In the present study, however, the required symmetries are apparently broken in two ways. First, the tube Reynolds number is ~ 1. Still, it may not be too unrealistic to ignore inertial forces since the corresponding particle Reynolds number is ~ 0.1. Second and perhaps more serious is the fact that the erythrocyte is of course not a rigid particle. In this work, radial migration would be manifest as a change in the period of rotation as the radial position and local shear varied. To date no such effect has been observed. Orbital migration would be observed for the case of oblate particles as a change in the pulse's relative maxima. Occasionally, I have observed pulses which suggest that this does in fact occur. These questions, however, require further investigation. Studies employing different tube geometries and flow rates and rigidly fixed erythrocytes are in progress.

VIII. CONCLUSION

The resistance pulse obtained by the passage of an insulating particle through a current-carrying pore depends on particle shape and orientation as well as volume. I have observed that for aspherical particles traversing a long pore and rotating in the shear of Poiseuille flow the resistance pulses exhibit a periodic amplitude variation.

The rotation of the particles is qualitatively well described by the theoretical results of Jeffery. For particles with an axis of symmetry theory indicates that all orbits include points where the axis of symmetry is perpendicular to the flow. If in addition the electrical shape factor (in particular the factor for the axis perpendicular to the field) is known then it is possible to accurately determine the particle volume.

In this paper I have discussed experiments with normal human erythrocytes. The data are consistent with the assumption that all cells have the electrical shape of an oblate ellipsoid of revolution and a diameter-to-thickness ratio of 4. The volume distribution of the cells is found to be a narrow normal distribution with a coefficient of variation of ~19%. This distribution is in agreement with those found by Shank et al. (18) (C.V. = 20%) and Miller and Wuest (19) (C.V. = 14%) who used a director to radially position the cells on the axis of a short orifice. I believe we can now be quite confident that normal human erythrocytes have a structureless gaussian volume distribution. The true volume distributions may be obtained using either the technique of Shank et al. and Miller and Wuest or the technique presented here.

Analysis of the data indicates that the cells enter the pore with their axis of revolution preferentially oriented perpendicular to the pore axis. Other questions of rheological interest have been briefly discussed. Finally, I observe that these resistance techniques may be of general utility in the study of small particle flow.

APPENDIX I

The shape factor equation can be writtten in terms of θ and Φ as

$$f = f_\perp + (f_\parallel - f_\perp) \sin^2 \theta \sin^2 \Phi. \tag{A 1}$$

The angle θ can be eliminated using the orbital Eq. 6 to yield

$$f = f_\perp + (f_\parallel - f_\perp) \sin^2 \Phi \frac{C_2^2}{C_2^2 + \gamma_E^2 \cos^2 \Phi + \sin^2 \Phi}. \tag{A 2}$$

We then see that the extrema determined by $df/d\Phi = 0$ are found at $\Phi = 0, \pm \pi/2, \pm \pi, \pm 3/2\, \pi \ldots$. For $\Phi = 0$ or any multiple of π substitution into Eq. A 2 gives

$$f = f_\perp, \qquad (\Phi = 0, \pm\pi, \pm 2\pi \cdots). \tag{A 3}$$

Likewise for Φ equal to any odd multiple of $\pi/2$ Eq. A 2 yields

$$f = f_\perp + (f_\parallel - f_\perp) \frac{C_2^2}{1 + C_2^2}, \qquad \left(\Phi = \pm\frac{\pi}{2}, \pm\frac{3}{2} \cdots\right). \tag{A 4}$$

For the case of an oblate ellipsoid of revolution $\gamma_E < 1, f_\perp < f_\parallel$ and Eq. A 3 describes the absolute minima whereas Eq. A 4 describes the relative maxima which depend on the orbital constant C_2. For a prolate ellipsoid $\gamma_E < 1, f_\perp > f_\parallel$ and Eq. A 3 describes the absolute maxima whereas Eq. A 4 describes the relative minima.

APPENDIX II

The minimum amplitude cumulative probability data of Fig. 9 is well described by the gaussian distribution,

$$P_1(A) = \frac{N}{\sqrt{2\pi}\sigma} \exp\left[\frac{(A - A_0)^2}{2\sigma^2}\right], \tag{A 5}$$

with $A_0 = 4.8$ and $\sigma = 0.9$. The normalization constant was determined so that area of the distribution was equal to the area of the minimum amplitude histogram of Fig. 8, viz., $N = 0.5 \times 119 = 59.5$. The distribution A 5 is for an orientation such that the shape factor $f = f_\perp$ and reflects a volume distribution with mean volume equal to $kA_0/f_\perp$ and standard deviation equal to $k\sigma/f_\perp$ where the constant k for this experiment is 18.6 μm^3 per amplitude unit. For different orientations we would obtain the following ditribution with the same coefficient of variation

$$P_1(A, f) = \frac{N}{\sqrt{2\pi\left(\frac{f}{f_\perp}\sigma\right)}} \exp\left[\frac{\left(A - \frac{f}{f_\perp}A_0\right)^2}{2\left(\frac{f}{f_\perp}\sigma\right)^2}\right]. \tag{A 6}$$

In section VI, I obtained the shape factor distribution for maximum amplitudes assuming initial orientations with $\Phi_0 = 0$ and θ_0 random, viz.,

$$P_2(f')\,df' = \frac{\gamma_B}{\pi} \frac{df'}{[\gamma_B^2 + (1 - \gamma_B^2)f']f'^{1/2}(1 - f')^{1/2}}, \tag{A 7}$$

where the reduced shape factor

$$f' = (f - f_\perp)/(f_\parallel - f_\perp). \tag{A 8}$$

Note that

$$\int_0^1 P(f')\,df' = 1.$$

To obtain the expected maximum amplitude distribution the convolution of Eqs. A 6 and A 7, i.e.

$$P_3(A) = \int_0^1 P_1(A, f)P_2(f')\,df', \tag{A 9}$$

was evaluated numerically to better than 1% accuracy. The result obtained with $\gamma_B = \gamma_H = 0.25$ is plotted in Fig. 8. In addition the cumulative maximum amplitude probability,

$$\frac{1}{N}\int_{-\infty}^{A} P_3(A)\,dA,$$

was also numerically evaluated and the result plotted in Fig. 9. Note that the adjustable parameters in this calculation are γ_H and γ_B, where γ_B fixes $f_\perp$ and $f_\parallel$. The parameters N, σ, and A_0 of distribution A 5 are fixed by the experimental minimum amplitude data.

This work has benefited on numerous occasions from discussions with C. P. Bean.
In addition, K. S. Cole has made useful comments.
I am grateful to M. V. Doyle and W. Healy for their careful assistance in the analysis of the experimental data.
I also wish to thank R. G. Miller and R. W. DeBlois for having informed me of the results of their work before publication.

A preliminary report on this work was presented at the 16th annual meeting of the Biophysical Society, February 1972.

Received for publication 10 July 1972.

BIBLIOGRAPHY

1. MAXWELL, J. C. 1904. *In* A Treatise on Electricity and Magnetism. Clarendon Press, Oxford, England. 3rd edition. **1**:440.
2. GREGG, E. C., and K. D. STEIDLEY. 1965. *Biophys. J.* **5**:393.
3. GROVER, N. B., J. NAAMAN, S. BEN-SASSON, and F. DOLJANSKI. 1969. *Biophys. J.* **9**:1398.
4. SMYTHE, W. R. 1964. *Phys. Fluids* **7**:633.
5. DEBLOIS, R. W., and C. P. BEAN. 1970. *Rev. Sci. Instrum.* **41**:909.
6. FRICKE, H. 1924. *Phys. Rev.* **24**:575.
7. VELICK, S., and M. GORIN. 1940. *J. Gen. Physiol.* **23**:753.
8. STONER, E. C. 1946. *Philos. Mag.* **36**:816.
9. OSBORN, J. A. 1945. *Phys. Rev.* **67**:351.
10. JEFFERY, G. B. 1923. *Proc. R. Soc. Lond. Ser. A Math. Phys. Sci.* **102**:161.
11. TREVELYAN, B. J., and S. G. MASON. 1951. *J. Colloid. Sci.* **6**:354.
12. BRETHERTON, F. P. 1962. *J. Fluid Mech.* **14**:284.
13. GOLDSMITH, H. L., and S. G. MASON. 1962. *J. Colloid. Sci.* **17**:448.
14. DAVIS, D. B., R. DULBECCO, H. N. EISEN, H. S. GINSBERG, and W. B. WOOD. 1970. Microbiology. Harper and Row, Publishers, New York. 345.
15. LUSHBAUGH, C. C., and D. B. HALE. 1964. Los Alamos Scientific Laboratory Report, 3034. 270–278.
16. UR, A., and C. C. LUSHBAUGH. 1968. *Brit. J. Haematol.* **15**:527.
17. BULL, B. S. 1968. *Blood.* **31**:503.
18. SHANK, B. B., R. B. ADAMS, K. D. STEIDLEY, and J. R. MURPHY. 1969. *J. Lab. Clin. Med.* **74**:630.
19. MILLER, R. G., and L. J. WUEST. *Ser. Hematol.* In press.
20. HARVEY, R. J. 1968. *Methods Cell Physiol.* **3**:1.
21. WEED, R. I., and A. J. BOWDLER. 1967. *Blood.* **29**:297.
22. GOLDSMITH, H. L. 1968. *J. Gen. Physiol.* **2**:5.